Kinetic lattice Monte Carlo simulations of interdiffusion in strained silicon germanium alloys

Renyu Chen[a] and Scott T. Dunham
Department of Electrical Engineering, University of Washington, Box 352500, Seattle, Washington 98195

(Received 26 June 2009; accepted 22 December 2009; published 3 March 2010)

Point-defect-mediated diffusion processes are investigated in strained SiGe alloys using kinetic lattice Monte Carlo (KLMC) simulation technique. The KLMC simulator incorporates an augmented lattice domain and includes defect structures, atomistic hopping mechanisms, and the stress dependence of transition rates obtained from density functional theory calculation results. Vacancy-mediated interdiffusion in strained SiGe alloys is analyzed, and the stress effect caused by the induced strain of germanium is quantified separately from that due to germanium-vacancy binding. The results indicate that both effects have substantial impact on interdiffusion. © *2010 American Vacuum Society.* [DOI: 10.1116/1.3294704]

I. INTRODUCTION

Fundamental modeling of diffusion in pure silicon as well as alloys is challenging as the time scales in which practical diffusion processes occur are significantly larger than the time scales that can be achieved by simulation techniques such as molecular dynamics (MD).[1] In contrast to MD approaches, kinetic lattice Monte Carlo (KLMC) simulations ignore atomic vibrations and treat diffusion as stochastic transitions between locally metastable states. Therefore, diffusion can be simulated with macroscopic system sizes and practical time scales. By replicating the sequence of atomic transitions and arrangements, KLMC provides an approach to fundamentally, yet efficiently, simulate atomistic diffusion processes.

In addition to the potential for simulating diffusion over a large time scale, KLMC proves even more useful for complicated diffusion mechanisms, such as stress-dependent interdiffusion in strained SiGe alloys. By replicating actual crystal structure, KLMC simulations can be used to predict diffusion and aggregation behavior that is not captured in continuum simulations or nonlattice kinetic Monte Carlo (KMC). This is particularly critical for SiGe alloys in which every lattice site has a different environment. Experiments[2,3] have been carried out to probe the interdiffusivity in SiGe alloys, but it is difficult to separate stress effects from alloy effects as required for general predictive models. KLMC can capture explicitly the local variations in alloy distribution and stress tensor and how they affect stochastic diffusion processes, therefore accurately predicting nanoscale atomic redistribution. This gives KLMC the potential for simulating stress-dependent interdiffusion in strained SiGe alloys.

In this article, we use a KLMC simulator to investigate vacancy-mediated Si–Ge interdiffusion in strained SiGe alloys. The simulations use an augmented discrete lattice structure and include the major atomic transition events taking place in the system. The inputs of the KLMC model, such as the activation energies for atomic hops and the induced strain values of point defects, are obtained from density functional theory (DFT) calculations summarized in previous works.[4–6]

[a]Electronic mail: renyu@u.washington.edu

II. MODELS

A. Simulation domain

The KLMC simulations consist of a large number of discrete sites on which atomic species can transition from one site and/or configuration to another. The unit cell of the domain is the crystalline silicon cubic structure, which consists of eight substitutional lattice sites. In addition, we augment the constituent sites to include high symmetry sites, which are involved in diffusion processes as listed in Table I. Illustrations of all these sites in one unit cell are shown in Fig. 1. The simulation domain includes a three-dimensional array of such cubic cells using three-dimensional periodic boundary conditions.

B. Atomic and point defect species

The atomic species that can be included in the system are silicon, germanium, and common dopants. Point defects include vacancies, intrinsic silicon self-interstitials, and extrinsic interstitials. From DFT calculations,[5] the most stable silicon self-interstitial structures are ⟨110⟩ oriented split interstitials Si(X) that occupy substitutional sites, and Si(H) interstitials that occupy hexagonal sites. Figure 2 illustrates a ⟨110⟩ split interstitial sitting on a substitutional site. We also consider germanium interstitials having similar structures, with Ge(H) being hexagonal interstitials and Ge(X) being ⟨110⟩ split interstitials. Note that the Ge(X) interstitial consists of one germanium and one silicon atom, not two germanium atoms.

C. Major transitions

In KLMC, a transition is a process in which an atom jumps from one site and/or configuration to another. Here, we only consider transitions that are associated with diffusion. There are two major categories of mechanisms for diffusion in Si, namely, vacancy and interstitial mechanisms.

TABLE I. Sites in the unit cell of the simulation domain and their numbers per cubic cell. A substitutional site is simply the silicon lattice site. A tetrahedral site is at the center of a tetrahedron formed by four substitutional sites. A hexagonal site is at the center of a hexagonal ring formed by six substitutional sites. A bond-centered site is at the center of a Si–Si bond. Lattice coordinates for typical substitutional, tetrahedral, hexagonal, and bond-centered sites are (0, 0, 0), (1/4, 1/4, 3/4), (5/8, 3/8, 3/8), and (1/8, 1/8, 1/8), respectively (see also Fig. 1).

Sites	Numbers
Substitutional (S)	8
Tetrahedral (T)	8
Hexagonal (H)	16
Bond-centered (B)	16

The vacancy mechanism involves a silicon-vacancy exchange process, while the interstitial mechanism involves a two step migration process denoted as $\mathrm{Si}(X) \rightarrow \mathrm{Si}(H) \rightarrow \mathrm{Si}(X)$.[5] In our analysis, we assume that the same diffusion mechanisms can be extended to germanium. Table II summarizes the transitions that are typical for self-diffusion in Si and/or interdiffusion in SiGe alloys.

For the interstitial $X \rightarrow H \rightarrow X$ mechanism, we take into account the orientation constraint, which implies that for the most energetically favorable transition the hopping directions and the split orientations are the most closely aligned. This limits the number of possible hops. For a ⟨110⟩ split interstitial, there are 12 neighboring hexagonal sites; however, for any specific split orientation, only 4 sites are accessible, 2 for each of the atoms forming the split interstitial.[5] Figure 3 shows the 12 hexagonal neighbors around a lattice site and the 4 accessible sites for the orientation pictured. Similarly, when a hexagonal interstitial hops to a substitutional site, the orientation of the resulting ⟨110⟩ split interstitial has only two choices.

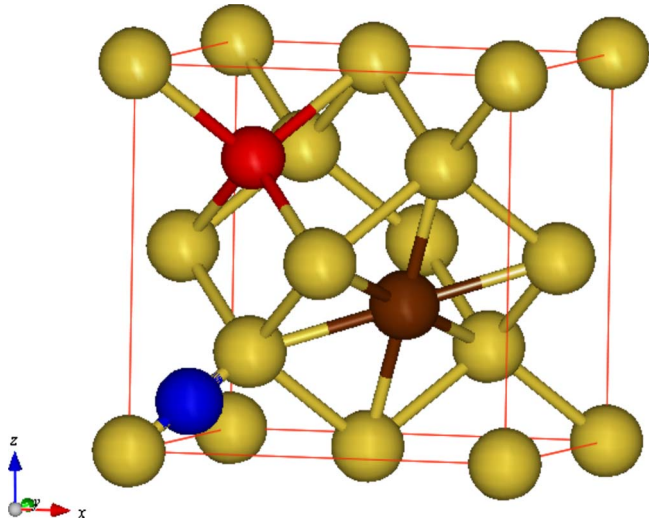

FIG. 1. (Color online) Illustration of sites in the unit cell of the simulation domain: substitution sites (light/yellow), a tetrahedral site (dark/red, upper left), a hexagonal site (dark/brown, right), and a bond-centered site (dark/blue, lower left).

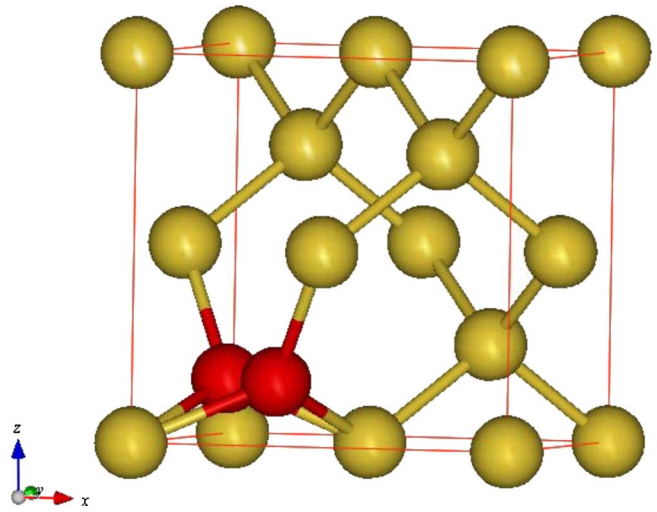

FIG. 2. (Color online) Illustration of a ⟨110⟩ split interstitial (dark/red, lower left).

D. System energies

The energy of the system is defined as follows:

$$E = E_f + E_b = \sum_i E_f^i + \sum_{i<j} \sum E_b^{i,j}, \tag{1}$$

where i and j run through all the defects and impurities in the system. The first term is the total formation energy of all species, which is dependent on the external stress. The formation energy of a species in the presence of an external applied stress $\boldsymbol{\sigma}$ is calculated as

$$E_f^i = E_{f0}^i - V_0(\Delta\boldsymbol{\varepsilon}^i \cdot \boldsymbol{\sigma}), \tag{2}$$

where E_{f0}^i is the formation energy under the stress-free condition, V_0 is the atomic volume of the silicon lattice, and $\Delta\boldsymbol{\varepsilon}^i$ is the induced strain of the point defects/impurities. Both stress and strain tensors are written in the contracted notation.[7]

The second term is the binding energy, which is a measure of the binding strength between a pair of defects/impurities. The binding energy is the sum of all pair energies of the system, extending from first nearest neighbors (1NNs) to nth nearest neighbors (nNNs). In our analysis here we simply consider interactions among 1NNs.

TABLE II. Hopping events and their associated stress-free migration barriers. S, X, and H denote a single atom on a substitutional site, a split interstitial on a substitutional site, and a single interstitial on a hexagonal site, respectively.

Hopping events	Notations	Forward barrier (eV)	Reverse barrier (eV)
Si diffusion-V (i)	$\mathrm{V}(S)+\mathrm{Si}(S) \leftrightarrow \mathrm{Si}(S)+\mathrm{V}(S)$	0.35	0.35
Si diffusion-I (ii)	$\mathrm{Si}(X) \leftrightarrow \mathrm{Si}(S)+\mathrm{Si}(H)$	0.34	0.25
Ge diffusion-V (iii)	$\mathrm{V}(S)+\mathrm{Ge}(S) \leftrightarrow \mathrm{Ge}(S)+\mathrm{V}(S)$	0.17	0.17
Ge diffusion-I (iv)	$\mathrm{Ge}(X) \leftrightarrow \mathrm{Ge}(S)+\mathrm{Si}(H)$	0.53	0.11
Ge diffusion-I (v)	$\mathrm{Ge}(X) \leftrightarrow \mathrm{Si}(S)+\mathrm{Ge}(H)$	0.47	0.25

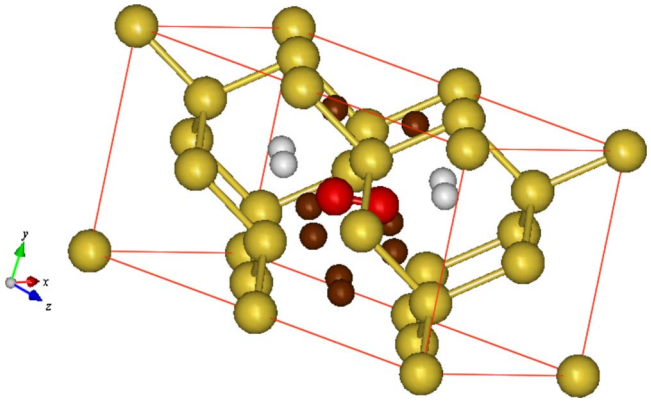

FIG. 3. (Color online) Twelve neighboring hexagonal sites (small spheres) of a [101] split interstitial (dark/red bonded pair, large spheres). The four light/gray ones are accessible sites and the eight dark/brown ones are not.

E. Transition rates

In KLMC, each transition is associated with three states, which are initial, transition, and final states. The rate of a transition is an Arrhenius function of the associated migration barrier E_m,

$$\nu = \nu_0 \exp(-E_m/k_B T), \tag{3}$$

where ν_0 is the attempt frequency and T is the system temperature. The migration barrier can be expressed as the sum of E_{m0}, an unbiased barrier, plus the change in the barrier due to other effects, such as pair binding and external stress. Table II lists the unbiased stress-free barriers of transitions included in this work, as obtained from DFT calculations.[4] The change in the migration barrier due to other effects can be expressed as a combination of the change in state energies that satisfies detailed balance[8]

$$E_m = E_{m0} + \left(\Delta E_{\mathrm{tr}} - \Delta E_{\mathrm{in}} + \frac{\Delta E_{\mathrm{fi}} - \Delta E_{\mathrm{in}}}{2}\right), \tag{4}$$

where ΔE is the change in state energies due to pair binding and applied stress, and the subscripts in, tr, and fi represent initial, transition, and final states, respectively. Tables III and IV are induced strain vectors used to calculate the change in the state formation energies via Eq. (2). The elapsed time Δt, for each hop, is calculated as the inverse of the summation of all possible transition rates,

TABLE III. Induced strain vectors of point defects/impurities which are associated with the energies of the initial and the final states of a hop. The induced strain for Si(X) and Ge(X) is orientation dependent. The table shows values for the [110] orientation.

	V(S)	Ge(S)	Si(H)	Si(X)	Ge(H)	Ge(X)
$\Delta\varepsilon_{xx}$	−0.22	0.05	0.20	0.26	0.25	0.31
$\Delta\varepsilon_{yy}$	−0.22	0.05	0.20	0.26	0.25	0.31
$\Delta\varepsilon_{zz}$	−0.22	0.05	0.20	0.05	0.25	0.10

TABLE IV. Induced strain vectors of the transition states of hops. The indices of hopping mechanisms are shown in Table II. Hopping mechanisms (ii), (iv), and (v) are orientation dependent. The table shows values for hopping vectors along [311].

	(i)	(ii)	(iii)	(iv)	(v)
$\Delta\varepsilon_{xx}$	−0.42	0.54	−0.37	0.59	0.59
$\Delta\varepsilon_{yy}$	−0.42	0.07	−0.37	0.12	0.12
$\Delta\varepsilon_{zz}$	−0.42	0.07	−0.37	0.12	0.12

$$\Delta t = \frac{1}{\Sigma_N \nu_N}, \tag{5}$$

where N runs through all possible transitions.

III. SIMULATIONS AND RESULTS

We have applied the KLMC simulation approach described above to investigate Si–Ge interdiffusion in strained SiGe alloys. Since the Si–Ge interdiffusion is predominately vacancy mediated,[9,11] we have carried out calculations on vacancy-mediated diffusion to see how stress and alloy concentration affect diffusion mechanisms. Generally, Ge has two effects on interdiffusion: one is the alloy effect due to Ge-V binding; the other is the stress effect. In the analysis below, a Ge-V binding of 0.31 eV has been included, which is obtained from DFT calculations.[6] Binding among other species are significantly lower (<0.13 eV) (Ref. 10) and are thus neglected in the simulation. To simplify the analysis, we treat all the stress-free formation energies as zero. To capture stress effects, we have included the induced strain vectors shown in Tables III and IV. These values are used to calculate the stress-induced changes in the formation energies, which, in turn, change transition rates. We assume that stress is only a function of Ge concentration. When calculating the stress, shear components can be neglected as they are zero for configurations considered, which results in a three-dimensional vector form

$$\boldsymbol{\sigma} = C \cdot \boldsymbol{\varepsilon}, \tag{6}$$

where C is the stiffness tensor of Si and $\boldsymbol{\varepsilon}$ is the external normal strain due to the presence of Ge atoms.

The structure that we have simulated is an epitaxial layer of pure Si grown on top of a relaxed $Si_{1-x0}Ge_{x0}$ layer. Generally, due to the positive induced strain of Ge atoms, the equilibrium lattice constant of $Si_{1-x}Ge_x$ is different from that of Si, a_0, with a relation given by[6]

$$a(x) = a_0 + 0.194x + 0.035x^2. \tag{7}$$

Considering the fact that the underlying SiGe layer is relaxed, the external strain of a point in the interface region with a Ge fraction of x is expressed as

$$\varepsilon_{\parallel}(x) = \frac{a(x) - a(x_0)}{a(x_0)},$$

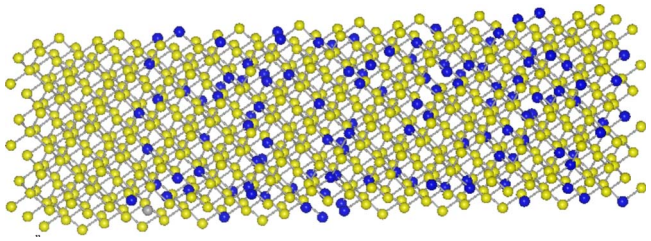

FIG. 4. (Color online) Initial configuration. Light/yellow and dark/blue spheres represent Si and Ge atoms, respectively. The left end represents pure silicon region and the rest represents SiGe with random alloy arrangement (Ge fraction equals 20%).

$$\varepsilon_{\perp}(x) = -\nu\varepsilon_{\parallel}(x), \tag{8}$$

where $\varepsilon_{\parallel}$ and $\varepsilon_{\perp}$ denote the strain components within and perpendicular to the interface plane, respectively, ν is Poisson's ratio, and x_0 is the germanium fraction in the underlying SiGe layer. Plugging Eq. (9) into Eq. (7) results in a biaxial tensile stress for the silicon and interdiffusion region.

To avoid clustering effects, simulations are carried out with a single vacancy present and then normalized for actual equilibrium vacancy concentrations. The vacancy is initially generated at a random location in the system. Vacancy mediates Si and Ge diffusion as described in Table II (no interstitial mechanisms are included as vacancy mechanisms generally dominate SiGe interdiffusion[9,11]). Initially, the Ge concentration profile is a step function, with a Ge fraction of 0 on one side and 20% on the other. Figure 4 shows an initial configuration of the SiGe alloy system, where Ge atoms are confined to the right side. Ge concentration in the domain is monitored as time proceeds. Our simulation temperature is 920 °C. Simulation is carried out for two cases: one that includes stress effects and the other that does not (no formation energy changes due to stress).

In our simulation, we initialize the system with one vacancy in a $5\times5\times64$ array of silicon unit cells. This implies that the vacancy concentration under the simulation condition is not necessarily the vacancy concentration under equilibrium conditions. In order to compare the simulated results with experimental data, the simulated results have to be scaled to yield behavior for equilibrium vacancy concentrations. In our analysis, we use free vacancy concentration, which is the vacancy concentration in the Ge-free region, to normalize the vacancy concentration since it can be readily compared to simple calculation. Once we determine the free vacancy concentration under the simulation condition, we can scale the result to equilibrium case. If the total elapsed time to reach the final profile is calculated to be t in the simulation, then the elapsed time to reach the same profile for the vacancy concentration under the equilibrium condition, t^*, is calculated as

$$t^* = \frac{C_V}{C_V^*}t, \tag{9}$$

where C_V^* and C_V are the free vacancy concentrations under the equilibrium and the simulation conditions, respectively. It can be seen that the elapsed time and the vacancy concentration have an inverse relation. This is consistent with the physical intuition that the higher the vacancy concentration, the faster the vacancy-mediated interdiffusion process, and thus the shorter time required to obtain a given profile. Another way to interpret this for $C_V^* < C_V$ (as in our simulations) is to think of the equilibrium case as if the system is attached to a huge reservoir which it equilibrates with. The difference between t^* and t represents the expected time during which the system is expected to not have any vacancies present, and thus no changes will occur in the system.

Before we proceed to the analysis of the equilibrium diffusivity as function of the Ge fraction, the determination of the free vacancy concentrations under both the equilibrium and simulation conditions should be elucidated. The free vacancy concentration under the equilibrium condition is a stress-dependent property and is closely related to the formation energy change due to stress,[5]

$$\frac{C_V^*(\vec{\varepsilon})}{C_V^*(0)} = \exp\left(-\frac{\Delta E_f^V(\vec{\varepsilon})}{kT}\right), \tag{10}$$

where $C_V^*(\vec{\varepsilon})$ and $C_V^*(0)$ represent the equilibrium free vacancy concentration with and without stress, respectively. $\Delta E_f^V(\vec{\varepsilon})$ is calculated from Eq. (2) with induced strain values of vacancy from Table III. $C_V^*(\vec{\varepsilon})$ corresponds to the equilibrium free vacancy concentration for the case where stress effect due to Ge is included, while $C_V^*(0)$ corresponds to that for the case where the stress effect is absent. Since we are not interested in their absolute values, the ratio in Eq. (10) is enough to make the comparison between the two cases.

To obtain the free vacancy concentration under the simulation condition, we calculate the free time ratio R as the ratio of the average time the vacancy spends on any one site in the Ge-free region to the total elapsed time

$$R = \frac{\bar{t}_0}{t} = \frac{(1/N_0)\Sigma_{i=1}^{N_0} t_i}{\Sigma_{i=1}^{N} t_i}, \tag{11}$$

where t_i is the cumulative time that vacancy is on site i during the simulation, N is the total number of sites in the simulation, and N_0 is the total number of sites in the Ge-free region. From the probability perspective, each site within that region has a probability of R to be occupied by a vacancy at any given time. Thus, the free vacancy concentration can be derived from the concentration of sites, C_s in that region, which is simply the silicon lattice site concentration (5×10^{22} cm^{-3}),

$$C_V = RC_s. \tag{12}$$

Thus, we are able to scale the results from Eqs. (10)–(12) and then perform Boltzmann–Matano analysis[12,13] of the system behavior under equilibrium vacancy concentration, which gives the diffusivity as

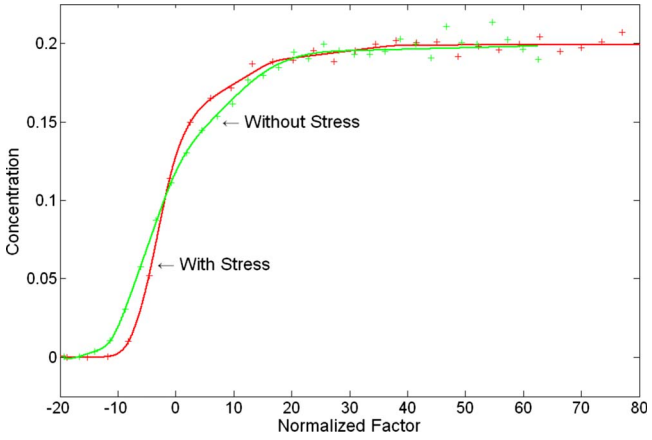

FIG. 5. (Color online) Diffusivity as a function of the normalization factor η for vacancy-mediated Si–Ge interdiffusion with and without consideration of the stress effect. The results are obtained for temperature equal to 920 °C. "+"s are original data and lines are fitted curves.

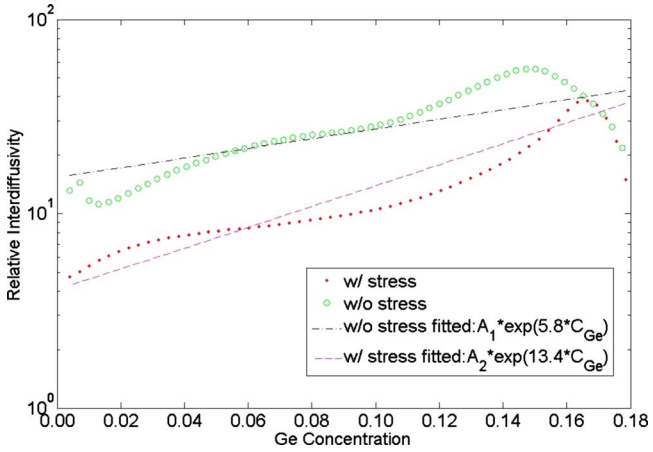

FIG. 6. (Color online) Data and lines fitted to Eq. (16) for pure alloy effect (w/o stress) and alloy effect combined with stress effect (w/stress) of Ge in the system. The results are obtained for a temperature of 920 °C.

$$D(C') = -\frac{1}{2t^*}\left(\frac{dz}{dC}\right)|_{C'}\int_0^{C'}(z - z_m)dC, \tag{13}$$

where z is the depth within the simulation, z_m is the Boltzmann–Matano plane defined in Ref. 2, t^* is time, and C is the Ge concentration. To factor out the time variable, we carried out the following substitution:

$$\eta = \frac{z - z_m}{\sqrt{t^*}}, \tag{14}$$

giving

$$D(C') = -\frac{1}{2}\left(\frac{d\eta}{dC}\right)|_{C'}\int_0^{C'}\eta dC. \tag{15}$$

Plotting diffusivity as a function of η for both cases allows us to compare the results directly. Figure 5 shows the calculated data and smoothed curve based on fitting to a constrained cubic spline function[14] for the Ge profile after simulation. Using the fitted curve, we can perform Boltzmann–Matano analysis which yields the diffusivity versus concentration relationship shown in Fig. 6. Fitting the data with an exponential relation between diffusivity and germanium concentration

$$D(x_{\mathrm{Ge}})/D_0 = \exp(Bx_{\mathrm{Ge}}). \tag{16}$$

we have extracted the fitted values of B for both alloy and stress effects of Ge in the system, which are shown in Table V. Thus, we have isolated the stress effect from the alloy effect, which indicates that under the simulation condition given above, stress and alloy effects have comparable sensitivity to the Ge concentration.

In our analysis, the exponential factor B of the total effect is extrapolated to be 13.4. This can be compared to the extracted values from Boltzmann–Matano analysis of experimental results[2] from Xia *et al.* In their paper, interdiffusivity is modeled in a piecewise exponential form with B of 8.1 and 23 in the tensile and compressive strain regime, respectively. Our analysis does not consider the different regimes of applied strain and gives a value that is close to the average of the two values in their paper. Also note that the extracted value of B under tensile strain in Xia *et al.*[2] appears to underestimate the experimentally observed dependence. Using a stronger Ge concentration dependence under tensile strain leads to extraction of a weaker dependence under compressive strain conditions, thus bringing both values closer to our result extracted from the simulation.

In general, Ge enhances V-mediated diffusion due to Ge-V binding, as Ge on neighboring sites lowers V formation energy. In addition, the lower concentration of Ge leads to tensile stress in the interdiffusion region that retards vacancy-mediated diffusion. Vacancies have a negative induced strain for the initial, final, and transition states, but the one for the transition state has a larger absolute value. A tensile stress will not only reduce the equilibrium vacancy concentration but also increase the formation energy difference between the transition state and the initial state, and therefore increase the migration barrier of the hop in Eq. (4), thus making vacancy-mediated migration less energetically favorable. This is consistent with Fig. 5, where the Ge profile is broader when stress effect is not present, which indicates that tensile stress on Si side retards vacancy-mediated diffusion.

IV. SUMMARY

We have presented kinetic lattice Monte Carlo simulations to investigate interdiffusion in strained SiGe alloys. The input values of KLMC including induced strains and migration barriers were obtained from DFT calculations. Simulation of

TABLE V. Fitted values of B in exponential model for SiGe interdiffusion due to different effects of the Ge concentration.

Stress effect	Alloy effect	Total effect
7.6	5.8	13.4

the SiGe alloy structure has separated stress and alloy effects caused by the presence of germanium. The application of KLMC approach to investigate diffusion processes indicates its potential for simulating full multistep annealing of nanodevices.

ACKNOWLEDGMENTS

This work was supported by the Semiconductor Research Corporation and Silicon Wafer and Defect Sciences (SiWEDS) consortium. Thanks are due to Chihak Ahn, Milan Diebel, and Blas Uberuaga for providing many of the DFT calculation results and to Maggie Xia for discussions regarding SiGe interdiffusion.

[1]G. Henkelman and H. Jonsson, J. Chem. Phys. **113**, 9978 (2000).
[2]G. Xia, J. L. Hoyt, and M. Canonico, J. Appl. Phys. **101**, 044901 (2007).
[3]P. Ranade, H. Takeuchi, W. C. Lee, V. Subramanian, and T. J. King, IEEE Trans. Electron Devices **49**, 1436 (2002).
[4]B. P. Uberuaga, Ph.D. thesis, University of Washington, 2000.
[5]M. Diebel, Ph.D. thesis, University of Washington, 2004.
[6]C. Ahn, Ph.D. thesis, University of Washington, 2007.
[7]R. M. Jones, *Mechanics of Composite Materials* (Scripta Book, Washington, 1988).
[8]A. Horsfield, S. T. Dunham, and H. Fujitani, Multiscale Modeling of Materials Symposium, 1999 (unpublished), p. 285.
[9]M. Gavelle *et al.*, J. Appl. Phys. **104**, 113524 (2008).
[10]C. Ahn, J. Song, and S. T. Dunham, "Transistor Scaling-Methods, Materials and Modeling," in *Material Research Society Symposium Proceedings*, 913, 2006, p. 179.
[11]I. Aberg, C. Ni Chleirigh, and J. L. Hoyt, ECS Proceedings: Advanced Gate Stack, Source/Drain and Channel Engineering for Si-Based CMOS: New Materials, Processes and Equipment, 2005 (unpublished), Paper No. PV2005–05, p. 505.
[12]L. Boltzmann, Ann. Phys. **289**, 959 (1894).
[13]C. Matano, Jpn. J. Phys. **8**, 109 (1933).
[14]P. Dierckx, Computing **24**, 349 (1980).